N72-10055

DEVELOPMENT AND FABRICATION OF LITHIUM-DOPED SOLAR CELLS

P. A. Iles
Centralab Semiconductor
Globe-Union Inc., El Monte, Calif.

I. INTRODUCTION

This paper outlines the progress made in the past year in the understanding and performance of lithium-doped solar cells.

II. SURVEY OF 1970 PRESENTATION

In the corresponding presentation a year ago (Ref. 1), the following achievements were reported:

(1) Improved boron diffusion methods, especially the use of reduced tack-on boron trichloride cycles, were developed. These methods had led to improved output from cells, especially when oxygen-lean silicon was used. Thus, the full capability of the several forms of silicon crystal growth was available for exploring a wide range of possible recovery times and degrees of cell stability.

(2) The lithium diffusion cycles used were predominantly with a single time cycle and with diffusion temperatures below 425°C, extending as low as 325°C.

(3) The cell output resulting from the combination of these boron and lithium diffusion methods was higher, as shown in Figs. 1 and 2, where the cumulative power distributions for JPL shipments C-11 and C-12 are shown.

(4) The lithium distribution throughout the cells was better understood by combining resistance probing, which gave the donor concentration in the bulk of the cell with capacitance-voltage analysis. This analysis explored the donor concentration very close to the PN junction. The distributions resulting from five different lithium diffusion schedules are given in Fig. 3 (bulk distribution) and Fig. 4 (distribution near the PN junction).

III. SURVEY OF WORK SINCE 1970

The work reported here has extended the results summarized in the foregoing in the following areas:

A. Cell Fabrication Sequence

The main fabrication steps required for cell fabrication (silicon growth, cutting, surface preparation, boron diffusion, lithium diffusion, contact application, coating application) have considerable interactions. Also the order of the fabrication processes can affect cell performance, often to a greater extent than anticipated. To illustrate the effects of the order, if contacts are applied to the front (boron diffused) P^+ surface before lithium diffusion, fairly severe heating cycles can be used to sinter the contacts. However, both these front contacts (and the antireflective coating, if present) can be attacked by lithium during its application and the diffusion cycle unless the lithium source is sufficiently diluted.

On the other hand, if the lithium is diffused first, there is no attack of the front contact and coating, and in addition, the P^+ layer can be

protected from possible interaction with the lithium. However, the range of sintering cycles available is now restricted to those which do not cause appreciable disturbance of the lithium concentration in the cell. Evaluation work reported by RCA (Ref. 2) showed good correlation between cell recovery time after irradiation, and the lithium concentration gradient near the PN junction. Thus, it is particularly important that the sintering cycles do not change this lithium gradient significantly.

Work in the past year has shown that it is possible to apply contacts and coating after lithium diffusion to obtain good electrical output and satisfactory contact adhesion by sintering for short times at temperatures less than the lithium diffusion temperature.

The effect of more severe sinter cycles on the lithium distribution is also being investigated quantitively.

B. Lithium Application

The paint-on lithium method provided well-controlled groups of cells (e.g., Figs. 1 and 2) despite apparent disadvantages in lack of uniformity. However, for consistency in larger scale fabrication of cells, vacuum evaporation of lithium metal was reevaluated. This reevaluation was prompted by several changes of cell design, all reducing some of the previous difficulties found with lithium evaporation. These favorable design changes included the need for less lithium in the cells than in previous years, and the use of lower lithium diffusion temperatures. Also the altered sequence described in the foregoing Subsection A, with contacts and coating applied last, allowed protection of the front cell surface during the lithium diffusion. Many of the cell groups prepared using lithium evaporation have shown satisfactory close distribution of cell parameters and lithium concentrations.

Some of the evaporated lithium groups had wide spread in all parameters. Systematic tests showed where the evaporation method was technique-dependent, and allowed greater control to be imposed. In analysis of these wide-range groups, the methods developed to test lithium distribution proved to be effective over the whole range.

C. Lithium Diffusion Cycles

This year's work has concentrated on the range of temperatures from 375 down to 325°C, with various times from 2 up to 8 h at these temperatures.

Two-stage diffusion cycles, e.g., those combining a tack-on followed by a redistribution cycle, are now considered to be inherently more difficult to control. First, the lithium concentration must be controlled on application; later the amount of the initial source left after tack-on must also be closely controlled. Also, these two-stage cycles often involve longer times at a given temperature than a single cycle, with more chance of variations occurring. At the lower lithium levels now being used, it is possible for the wide spread in lithium characteristics during the two cycles to be masked by the general improvement in cell characteristics. In other words, the cell performance before irradiation may be relatively insensitive to the differences in lithium distribution. In addition, tests using thin slices (approximately 7 mils) showed that the redistribution cycle could lead to severe cell degradation as a result of excess lithium present in the PN junction depletion region, although the average lithium level was low throughout the N region.

D. Lithium Distribution

More information and insight has been added to the way in which the lithium is distributed and the resultant effects on cell properties.

1. Surface concentration (C_s). The buildup of the lithium concentration at the back surface where the lithium was applied, was measured as a function of time at various temperatures.

Figure 5 shows the measured values. Qualitatively, the results are as expected, with a gradual buildup of C_s for longer times, to a maximum value – the rate of increase and the maximum value being higher for higher temperatures.

Two other features were noted. First, the buildup was slower than expected, often requiring around one hour to reach the maximum C_s value. Second, after the saturation region, C_s decreased for longer diffusion times. The points shown on Fig. 5 for times greater than 2 h are those calculated for the C13 cells, discussed in Section E1 following.

2. Concentration near the PN junction. Theoretically, both the lithium concentration and its gradient at any plane in the cell, including the important region near the PN junction at the front of the cell, are both directly proportional to C_s. However, as Figs. 3 and 4 showed the lithium concentration gradient near the junction must be much increased over the theoretical value in order to give concentrations which agree with those calculated from C-V measurements. Gradients up to seven times the theoretical value have been measured. The cause of this increase and the associated lower concentration at the junction are believed to be the perturbation of the theoretical lithium distribution by the electric field in the junction depletion region, which assists the flow of lithium into the P^+ layer.

The changes in lithium distribution were followed by measurements on samples diffused at a given temperature for several different times. Figure 6 shows the results of such a test. The lithium buildup at the PN junction was followed by capacitance measurements. For the three shorter times, no measurable increase at the junction was observed in keeping with the theoretical curves shown. The two longer times are seen to give increases in lithium near the junction. The changes needed in the theoretical distribution are shown by the dotted lines. Good consistency between measured and theoretical lithium distributions was obtained if the dotted line changes occurred over a distance around 20 μm.

3. Changes in concentration with diffusion time. The trend noted in the foregoing Subsection D(1) for the C_s value at a given temperature to decrease steadily with diffusion time gave

increased spread in C_s values. This, in turn, led to increased spread toward lower values of lithium concentrations and gradient near the junction. Although the cause of these changes was first sought in effects near the junction, the C_s measurements showed that the likely cause was the decrease in C_s resulting from depletion of the lithium source.

This depletion can be reduced by controlling the amount of lithium deposited or by modification of the diffusion procedure to minimize losses. In the following Subsection E2 the cell parameters resulting from wide variation in C_s are compared to the tighter grouping obtained when the lithium source depletion was reduced.

E. JPL Shipment C13

This shipment consisted of ten groups, each with thirty cells. The lithium diffusion schedules used were between those used for C11 and they are shown in Table 1. At each diffusion temperature, the lithium was applied to batches of slices and the diffusion was performed on a split boat, allowing withdrawal of the shorter time group first, leaving the longer time group in the furnace. The differences in cell properties for both short and long time diffusions showed more correlation with the separate batches, showing that the main variable was in the paint-on lithium application. The fabrication sequence applied front contacts and coating before lithium diffusion.

In general, the cells showed good control and good I-V performance. The controlling variable was the diffusion time. Figure 7 shows the average values of P_{max}, V_{oc}, I_{sc}, and capacitance for the thirty cell groups in C13. P_{max} varies over about 4%. V_{oc} and I_{sc} show slightly larger ranges (up to 5.5%) but their out-of-phase variations led to reduced spread in P_{max}. Also V_{oc} and capacitance vary in phase, the spread in capacitance being up to 30%.

Figures 8 and 9 show in more detail some of the parameters for the C13 groups. In these figures, average values and the spread in the groups for P_{max}, V_{oc}, capacitance, and donor concentration gradient near the junction are plotted as a function of increasing diffusion time. The P_{max} values are satisfactorily high and tightly grouped. The other parameters all show a trend toward lower values and larger spreads at the longer time. These two figures show that the I-V characteristics can have small spread, but may be associated with larger spread in the lithium concentration or its gradient.

Figure 10 plots the cumulative percentage of P_{max}, averaged for all 300 cells in C13 with the upper and lower thirty cell groups shown also. For comparison, the distribution for C12 is given. This figure shows that the general level of cell output was good.

Figure 11, for ten cells in C13G and C13H shows good correlation between V_{oc} and the lithium concentration and concentration gradient near the junction, calculated from capacitance measurements. For C13G, the shorter time diffusion, the grouping is tighter and both V_{oc} and the lithium parameters are higher. Even for cells with less lithium, the V_{oc} values are generally high, and this figure shows that greater resolution of the underlying correlations is now feasible.

Figure 12 plotted for 100 cells, ten in each C13 group, shows that V_{oc} is approximately proportional to the logarithm of the lithium concentration. The estimated slope of the curve is approximately 0.026 V^{-1}, a value expected if the PN junction is operating at current levels where it approaches diode diffusion theory operation. The total spread in V_{oc} is around 5%, whereas the total spread in concentration is 400%.

Table 2 lists the values of surface concentration calculated for each of the C13 groups. These C_s values were obtained by combining the lithium concentration and concentration gradient near the PN junction (estimated from C-V methods). Assuming the gradient occurred for a distance of 20 μm from the junction, a value of lithium concentration was obtained at this 20-μm plane. Then the theoretical distribution was extrapolated from this plane to the back surface to give the C_s value. The groups in Table 2 are plotted in increasing order of diffusion time, and show the steady fall-off of C_s.

In summary, C13 provided 300 cells of good output, but with sufficient differences between the groups to show that diffusion time was a more important controlling parameter than had been suspected earlier. To reduce the effects of source depletion at the longer times, a later shipment (C15) was planned to include both paint-on and evaporated sources, to check that the source depletion was reduced for the more concentrated source.

1. JPL shipment C14. The intention in C14 was to compare oxygen-rich (C.G.) silicon and oxygen-lean (Lopex) silicon in two of the lower temperature single time cycles. Also lower resistivity Lopex silicon (15 Ω-cm) was used to check if the five-fold increase in background concentration was of advantage for higher fluence irradiations. The fabrication sequence for C14 applied lithium before any contacts or coatings were present. Table 3 gives details of the silicon and lithium cycles used.

Figure 13 gives the average values and the spread of P_{max}, V_{oc} and capacitance for the C14 groups. The general level of P_{max} (and V_{oc}) was good. For a given lithium cycle, the C.G. silicon cells had higher V_{oc} (and I_{sc}) than the Lopex cells. However, this higher V_{oc} was accompanied by the lower capacitance (and thus lower lithium concentration near the junction) usually found for C.G. silicon. This lower capacitance can explain the higher I_{sc} values obtained for C.G. silicon, but does not explain the V_{oc} differences. In this case, the differences in silicon grown by the two methods have more effect on I-V characteristics than the differences obtained in lithium concentration.

2. JPL shipment C15. The purpose of C15 was to compare three different silicon ingots using either paint-on or evaporated lithium sources for each group and a diffusion schedule similar to those used in C13. A schedule of 350°C for 240 min was chosen; and in addition, a group of C.G. cells was fabricated using the evaporated source and 350°C for 480 min to check if the lithium depletion was reduced for the longer diffusion time.

Table 4 shows details of the C15 groups.

Figure 14 plots the average values and the spread for the various C15 groups. Again, the overall level of P_{max} is good and, as seen in C11 and C14, the P_{max} values for C. G. silicon are slightly higher than those for Lopex cells. There is no significant difference in these preirradiation measurements between the medium and high resistivity Lopex groups. Also, as for C14, the lithium concentration near the PN junction, as measured by capacitance, was higher for the Lopex ingots.

The overall spread is not markedly lower for the lithium evaporation groups, possibly because the diffusion time is not long. However, the spread in P_{max} and especially in capacitance for the 8-h diffusion group C15G was much lower than obtained for the longer time C13 groups. This shows that lithium depletion has been minimized by the more concentrated source.

During fabrication of the evaporated lithium groups, some batches showed signs of severe lithium depletion. These signs included both serious reduction in V_{oc} (with accompanying higher I_{sc}) and low capacitance values often near the level found for cells made with no lithium. Resistance probe measurements showed that the lithium concentration was much reduced for these batches. These tests showed that lithium evaporation was technique dependent. Using improved techniques mainly in reducing the interaction of lithium and silicon before the slices were placed in the diffusion furnace, gave increased lithium concentrations with very closely grouped sets of parameters. Figure 15 compares the spread of three cell parameters, V_{oc}, capacitance and P_{max} for three different conditions of lithium application — namely paint-on, lithium evaporation with varying interaction, and well-controlled lithium evaporation. The silicon used for these three tests was the same (Lopex, 75 Ω-cm) as was the lithium diffusion schedule at 350°C for 240 min. The paint-on source again shows tight grouping of P_{max} and V_{oc} with a wider spread in capacitance. The less controlled evaporation group had lower values for P_{max}, V_{oc}, and capacitance with wide spreads. The well-controlled evaporation group had high values with small spread for all parameters.

F. More Complex Structures

The present design of lithium cell with suitably chosen silicon and lithium diffusion conditions can give cells with good performance for many possible missions. Any further complexity added to the cell design must be justified by the more severe conditions imposed by particular missions.

The study of two of the possible complexities needed to maintain cell stability following high fluence irradiation has been continued this year.

1. Use of additional N^+ layer at the back surface. This layer, using donors other than lithium, has been used particularly with oxygen-lean silicon to reduce the back contact resistance. However, as will be noted in the following Subsection G1, present contact resistances are satisfactorily low. More tests are needed to check the threshold fluence at which carrier removal by lithium depletion (occurring during the recovery phase following irradiation) increases the contact resistance appreciably.

2. Use of additional N^+ layer near the front surface. Past results have shown that this layer can increase the stability of the PN junction when lithium carriers are removed following high fluences. Again tests are needed to find the threshold fluence which makes this N^+ layer necessary. The threshold fluence will be higher as the starting donor concentration is increased. Thus comparison of the C15 Lopex groups will be of interest.

The other possible use of the front surface N^+ layer is to control the final distribution of lithium near the PN junction after the lithium diffusion cycle. Tests in progress will show if any advantageous distributions can be obtained.

3. Front surface introduction of lithium. In the past year, tests continued on the possible merits of introducing lithium through the front surface of both P/N and N/P cells. The cells made to date with this method did not show any advantages over the conventional design cells.

G. Other Topics

1. Contacts. For the levels of lithium used in the past year, Ti-Ag contacts have given curve fill factors (CFF) values between 0.70 and 0.76. The sequence used for shipment C13 (front contacts applied before lithium) generally gave CFF around 0.72. The later shipments C14 and C15, where both contacts were applied after lithium diffusion, had CFF around 0.74 with minimum lithium depletion at the back surface, CFF > 0.75 have been obtained. This lessens the need for an extra N^+ layer at the back surface to reduce contact resistance.

Evaluation of various contact sintering cycles is in progress. The cycles will be compared for adhesion of the contacts, the effects on the I-V characteristics of the lithium cells, and the effects on lithium distribution within the cells.

2. Improved antireflective coatings. Improved coatings, using double layers of dielectrics have given slight increase (2%) in the output of lithium cells. The increase was less than that obtained on N/P cells because present lithium cells already have a form of double-layer coating.

3. Maximum output versus lithium concentration. A search was made for the highest P_{max} values obtained for different lithium concentrations near the PN junction. The curve joining the pairs of corresponding points for all the cells measured is given in Fig. 16. For lithium concentrations around 5×10^{14} cm^{-3}, P_{max} = 33 mW is possible for 2-cm^2 cells. 31 mW was obtained for 10^{15} lithium atoms cm^{-3} for C. G. silicon, and for $>10^{15}$ lithium atoms cm^{-3} for Lopex silicon. This figure shows the current feasibility of reaching an optimum trade off between P_{max} and recovery characteristics.

IV. SUMMARY

This year has shown further improvement in the performance and understanding of lithium cells.

They have proved to be superior to N/P cells for several possible missions, particularly when energetic heavy particles (protons or neutons) are a significant fraction of the bombarding particles. The high output and repeatability are obtainable from both oxygen-rich and oxygen-lean silicon. The precision of analysis of cell behavior has been improved.

The analytical techniques developed will allow even further control of the lithium distribution, aiding in closer grouping of both pre- and post-irradiation performance.

The fabrication sequence alterations have led to higher cell output, better appearance, and increased contact strength.

The present methods of fabrication and analysis are well suited to beginning the evaluation of possible pilot-line scaling up.

There is still a need for a figure of merit to allow assessment of the radiation capability of the cells. Before lithium cells are used in large numbers, they must pass a relatively simple test to prove that all the cells on the array will degrade and recover in a similar fashion. At present, the test suggested by RCA (Ref. 2), wherein the lithium concentration gradient is measured, provides the best figure of merit, but further tests are necessary.

As shown in Fig. 15, there is still some room for improvement in the cell output for a given lithium concentration. It will be of interest to see if other papers on irradiation effects substantiate the optimism that the cell fabricators have regarding lithium cells.

REFERENCES

1. Iles, P. A., "Progress Report on Lithium-Diffused Silicon Solar Cells" in Proceedings of the Third Annual Conference on Effects of Lithium Doping on Silicon Solar Cells, Jet Propulsion Laboratory, Pasadena, Calif., April 1970.

2. Faith, T. J., Corra, J. P., and Holmes-Siedle, A. G., "Room Temperature Stability and Performance of Lithium-Containing Solar Cells – An Evaluation," in the Conference Record of the Eighth IEEE Photovoltaic Specialists Conference, Seattle, Wash., August 1970.

ACKNOWLEDGMENT

We would like to thank NASA and JPL for their support under Contract No. 952546 and Mr. Paul Berman for his technical support.

Table 1. Lithium diffusion schedules for C11 and C13

Cell group	Diffusion temperature, °C	Diffusion time, min
C11A	325	480
C11B	325	480
C11C	325	480
C13A	330	180
C13B	330	420
C13C	340	180
C13D	340	420
C13E	350	300
C13F	350	300
C13G	360	180
C13H	360	420
C13I	370	240
C13J	370	360
C11D	375	180

Table 2. Surface concentration of lithium for C13 groups

Cell group	Temperature, °C	Time, min	Calculated C_s, cm^{-3}
C13A	330	180	1.3×10^{17}
C13C	340	180	1.7×10^{17}
C13G	360	180	1.6×10^{17}
C13I	370	240	0.95×10^{17}
C13E	350	300	1.2×10^{17}
C13F	350	300	1.2×10^{17}
C13J	370	360	0.75×10^{17}
C13B	330	420	0.70×10^{17}
C13D	340	420	0.50×10^{17}
C13H	360	420	0.65×10^{17}

Table 3. Details of JPL shipment C14

Cell group	No. of cells	Silicon used	Lithium diffusion
C14A	30	Lopex – 15 Ω-cm	Paint on at 375 °C for 180 min
C14B	30	C. G. – 30 Ω-cm	Paint on at 375 °C for 180 min
C14C	30	Lopex – 15 Ω-cm	Paint on at 350 °C for 300 min
C14D	30	C. G. – 30 Ω-cm	Paint on at 350 °C for 300 min

Table 4. Details of JPL shipment C15

Cell group	No. of cells	Silicon used	Lithium diffusion
C15A	30	Lopex – 15 Ω-cm	Paint on at 350 °C for 240 min
C15B	30	Lopex – 15 Ω-cm	Evaporated at 350 °C for 240 min
C15C	30	Lopex – 75 Ω-cm	Paint on at 350 °C for 240 min
C15D	30	Lopex – 75 Ω-cm	Evaporated at 350 °C for 240 min
C15E	30	C. G. – 30 Ω-cm	Paint on at 350 °C for 240 min
C15F	30	C. G. – 30 Ω-cm	Evaporated at 350 °C for 240 min
C15G	30	C. G. – 30 Ω-cm	Evaporated at 350 °C for 480 min

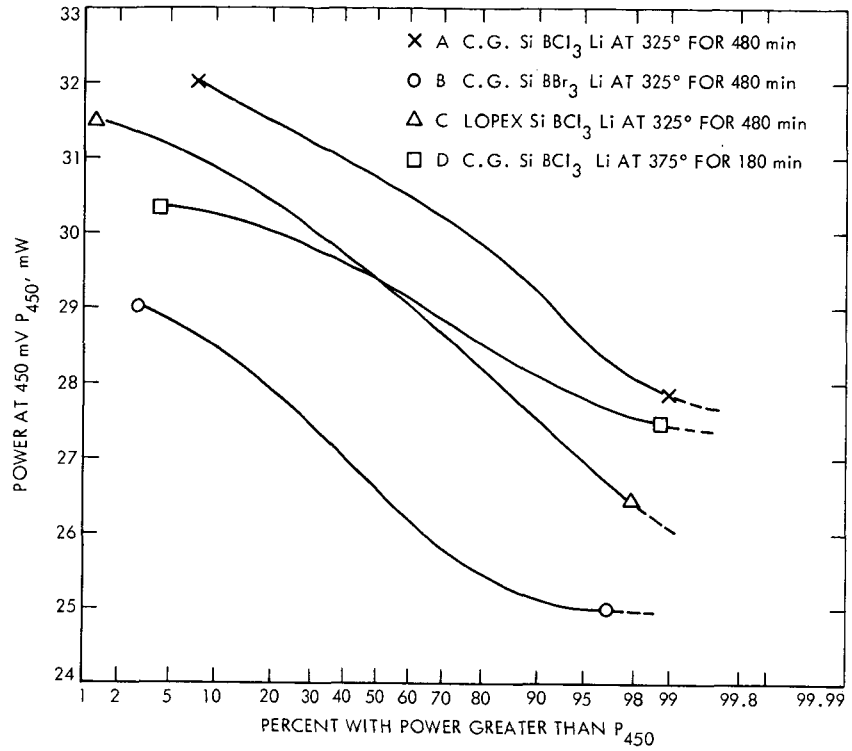

Fig. 1. Cumulative P_{max} distribution for JPL shipment C11

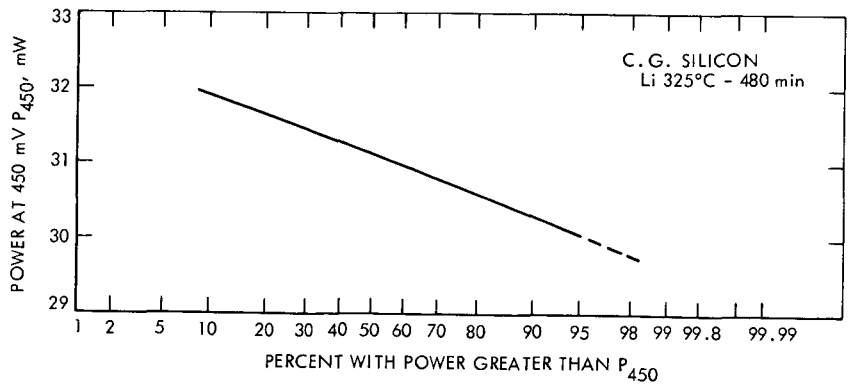

Fig. 2. Cumulative P_{max} distribution for JPL shipment C12

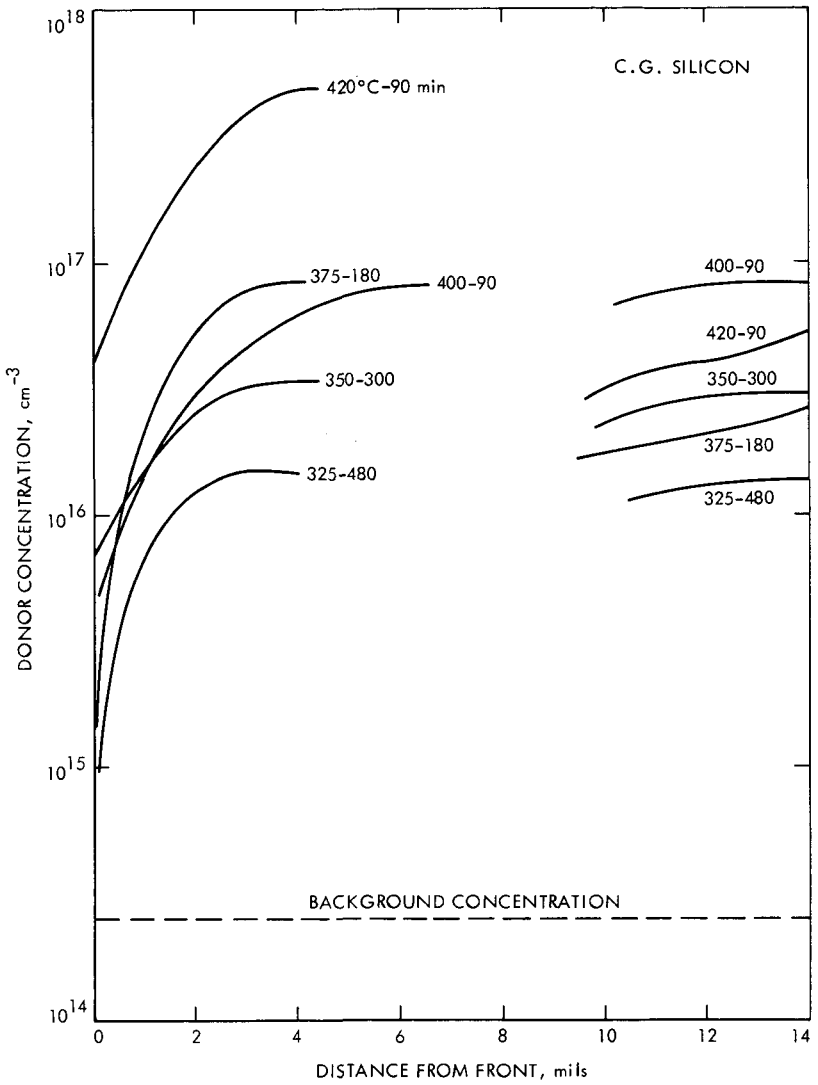

Fig. 3. Donor concentration profiles (in the bulk) for various lithium diffusion schedules

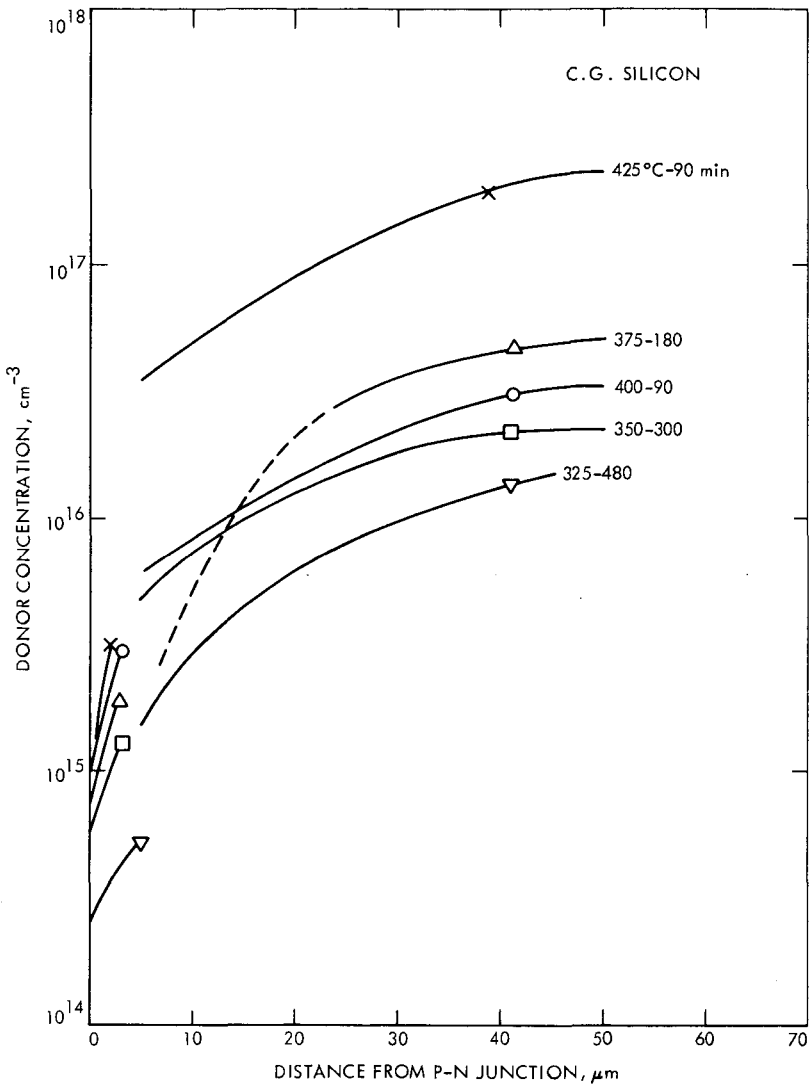

Fig. 4. Donor concentration profiles (near the P/N junction) for various lithium diffusion schedules

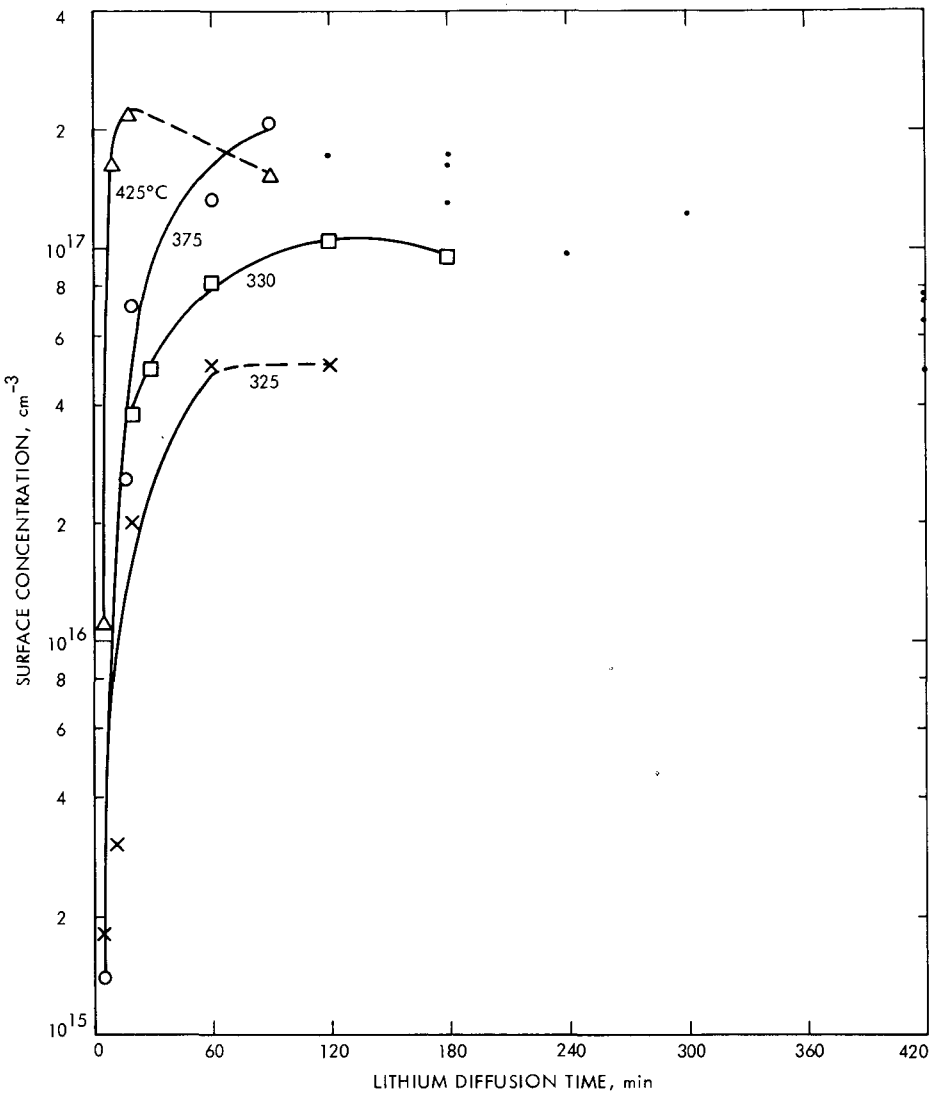

Fig. 5. Build-up of surface concentration of lithium for increasing time at various temperatures

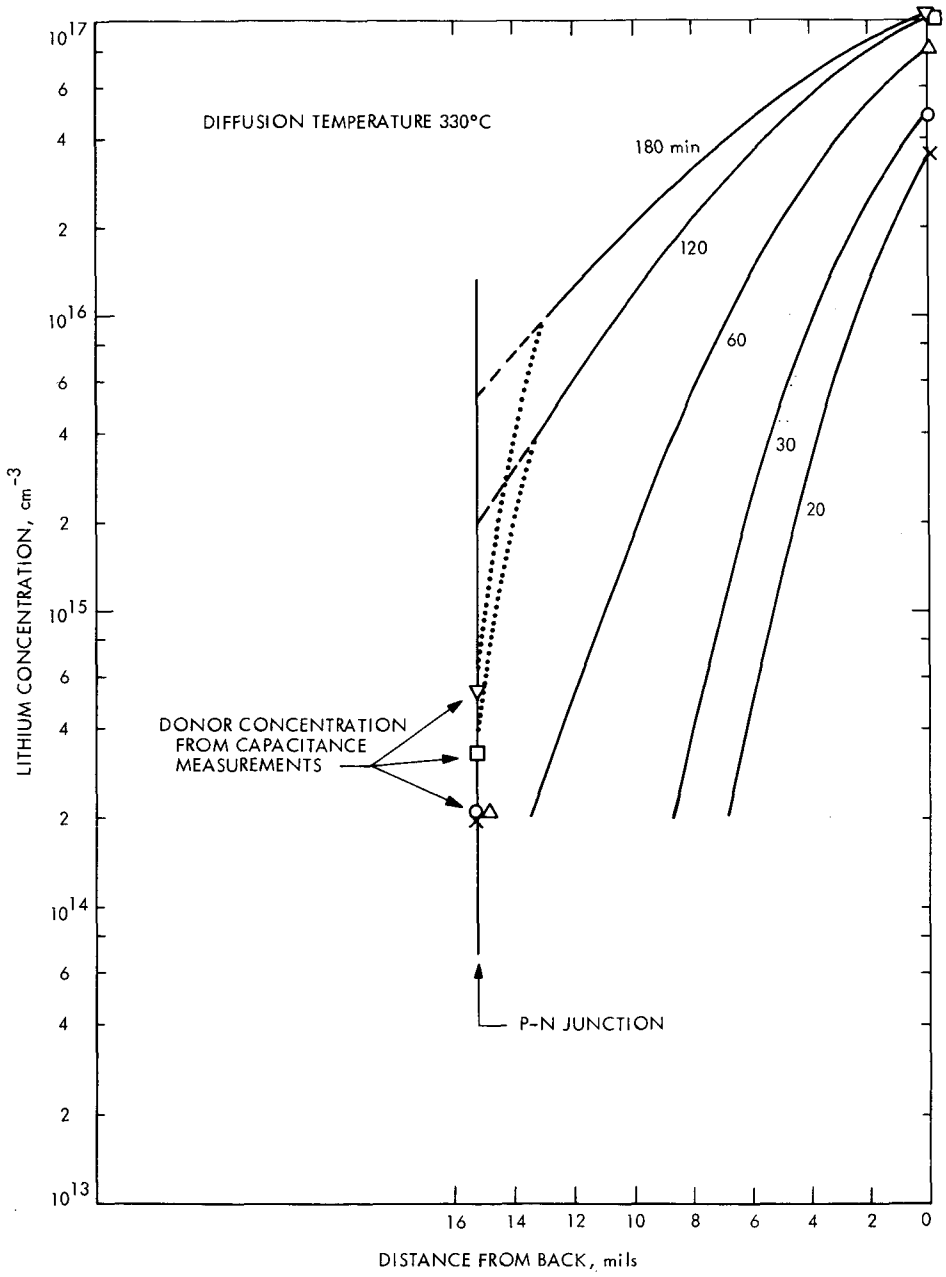

Fig. 6. Changes in lithium concentration profile and the values measured at the P/N junction as the diffusion time at 330°C was increased

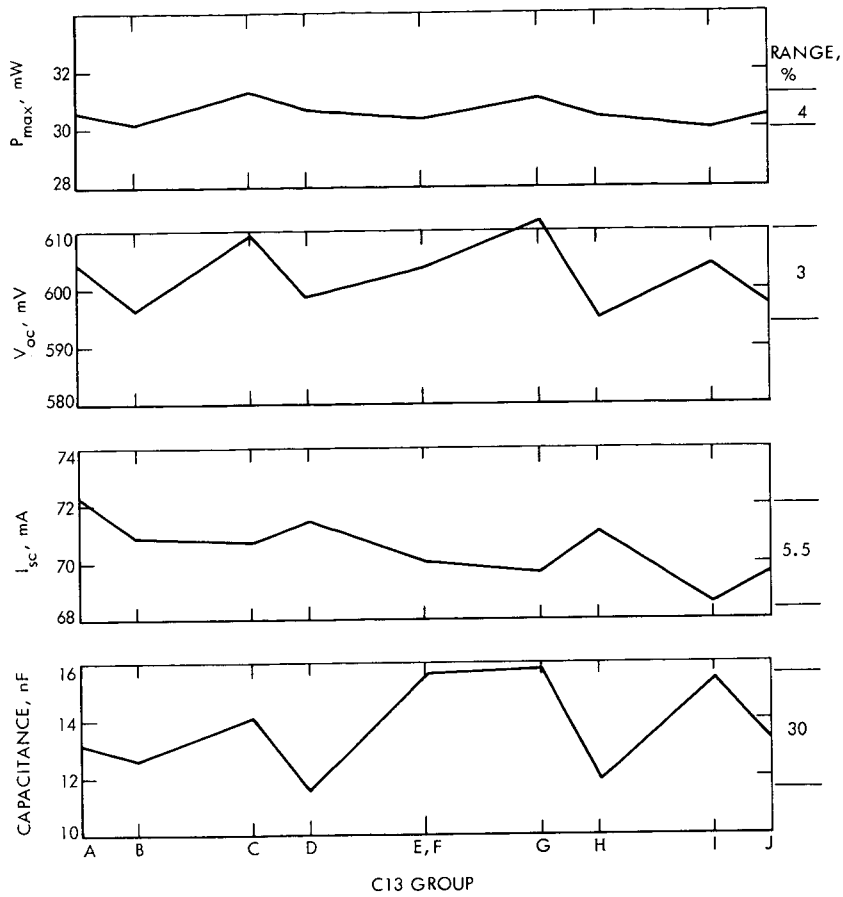

Fig. 7. Average values for P_{max}, V_{oc}, I_{sc}, and capacitance for the ten C13 groups

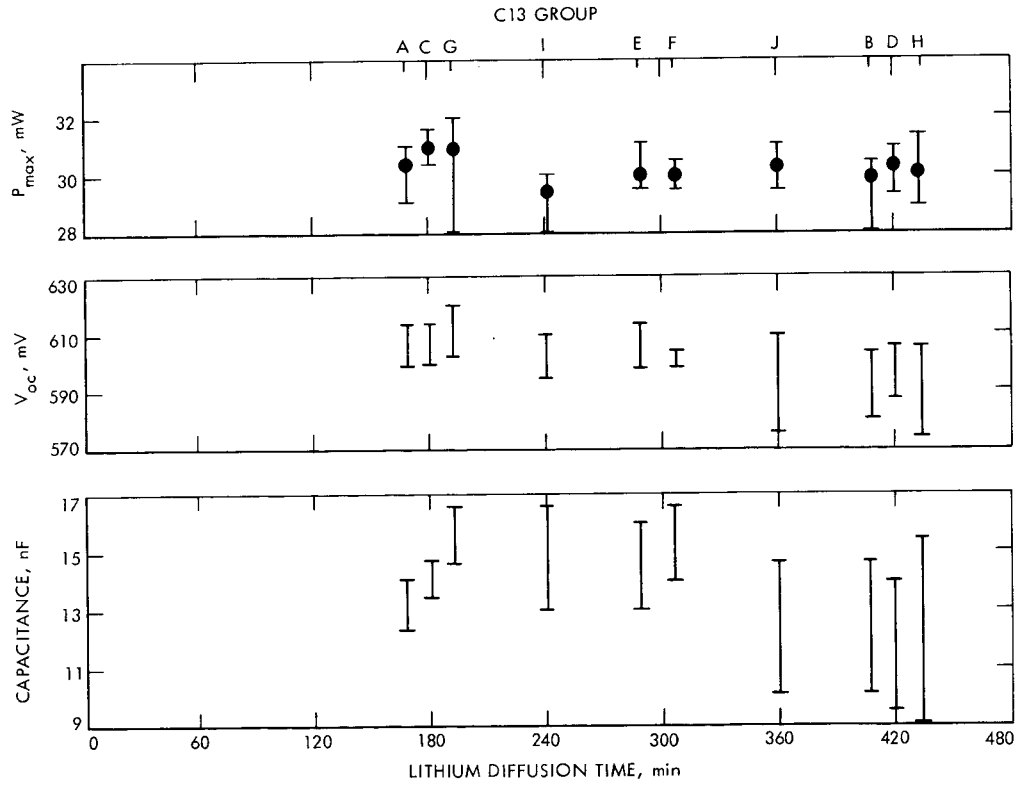

Fig. 8. Average values and spread for P_{max}, V_{oc}, and capacitance for the C13 groups, plotted as a function of diffusion time

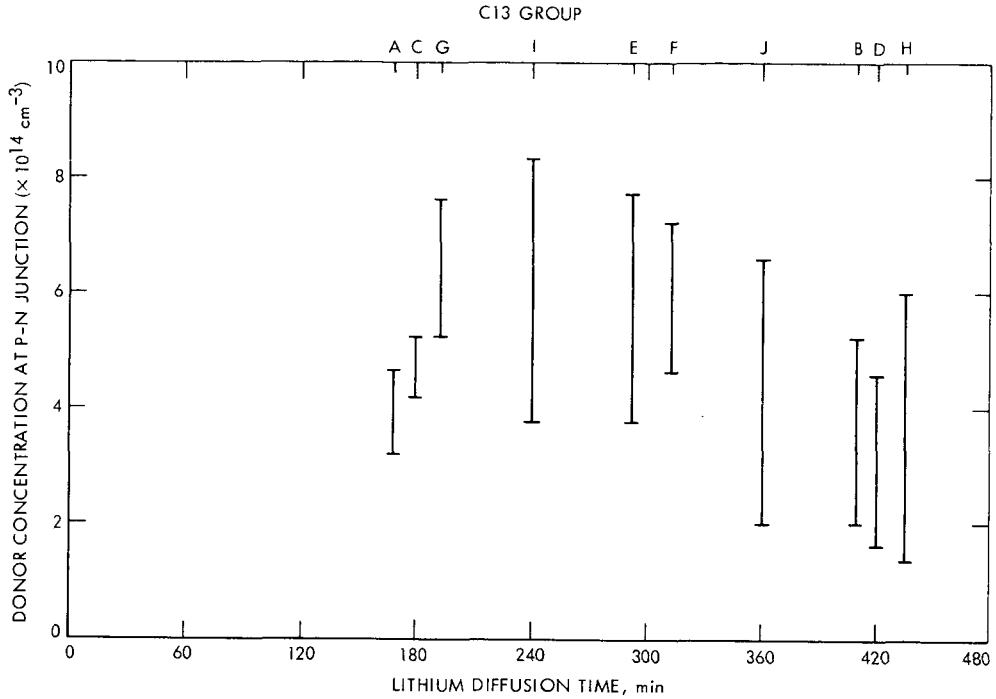

Fig. 9. Average values and spread of donor concentration gradient at the P/N junction, for the ten C13 groups, plotted as a function of diffusion time

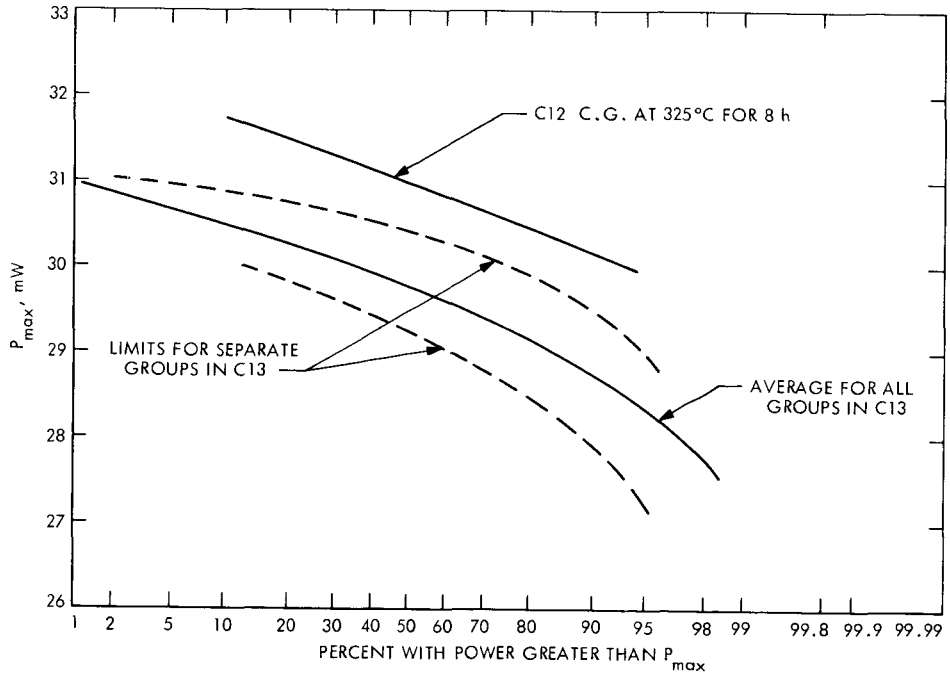

Fig. 10. Cumulative P_{max} distribution for total and extreme groups in C13 (C12 shown for comparison)

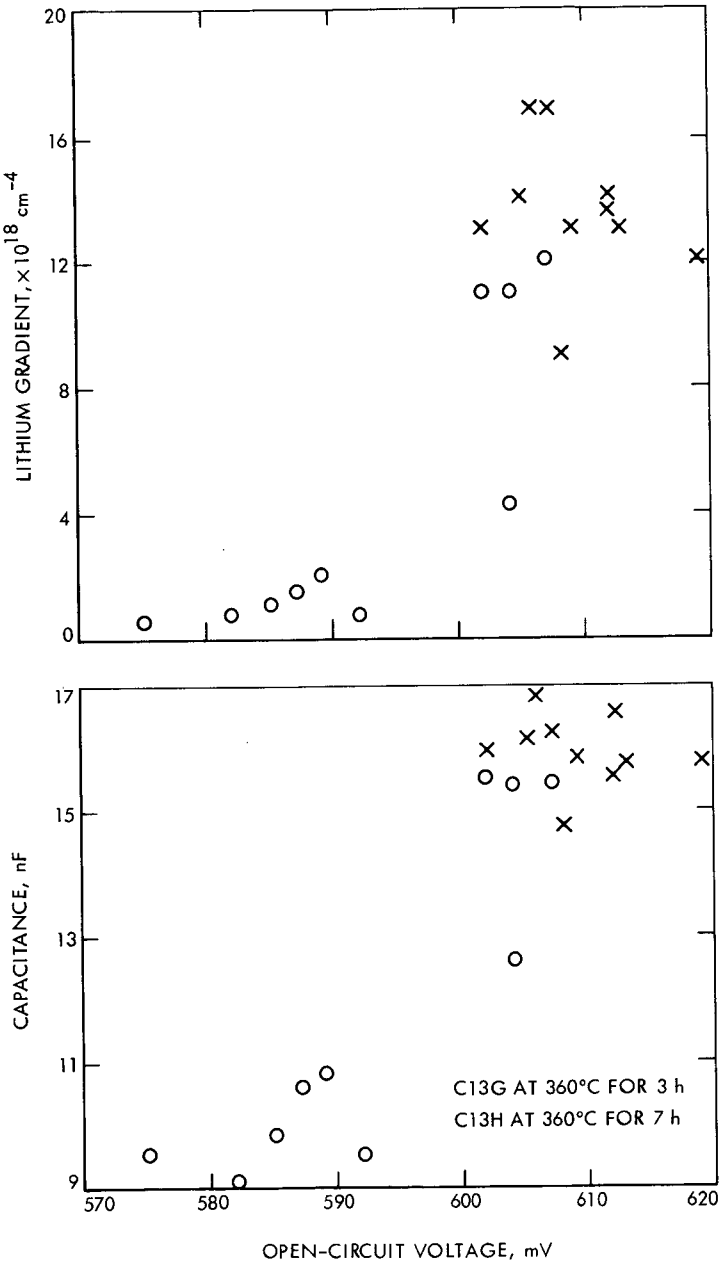

Fig. 11. V_{oc} plotted versus capacitance and lithium concentration gradient near the junction for two 10-cell groups in C13

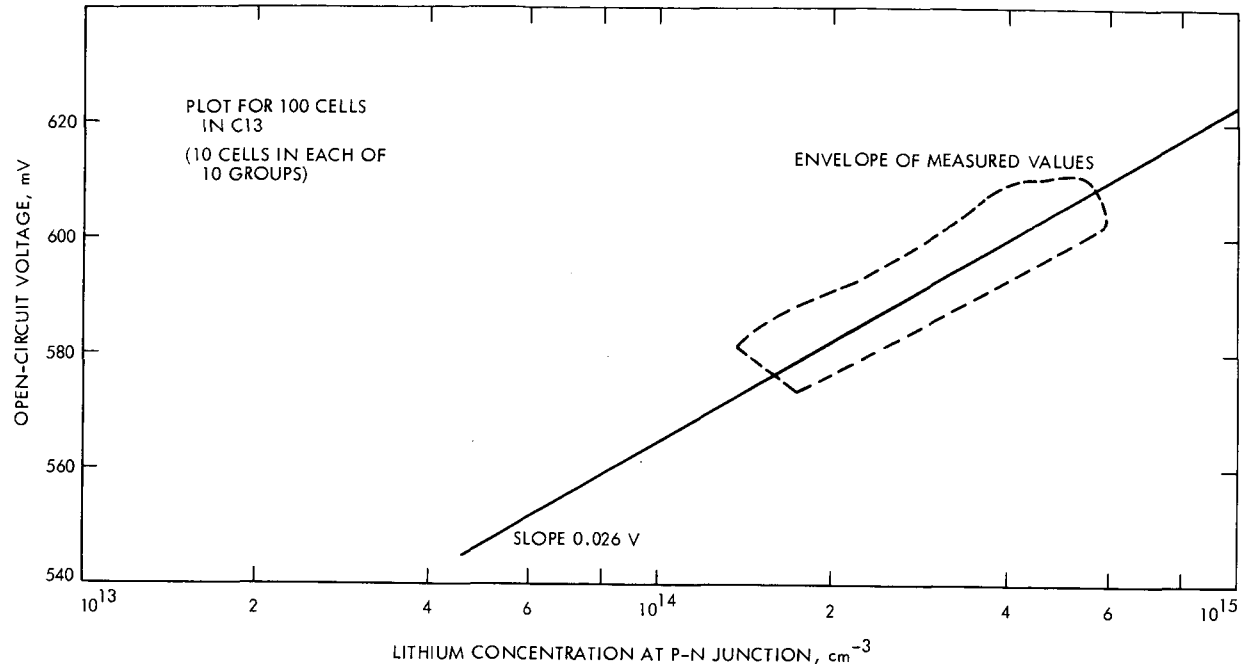

Fig. 12. V_{oc} plotted against logarithm of the donor concentration for 100 cells, 10 in each C13 groups

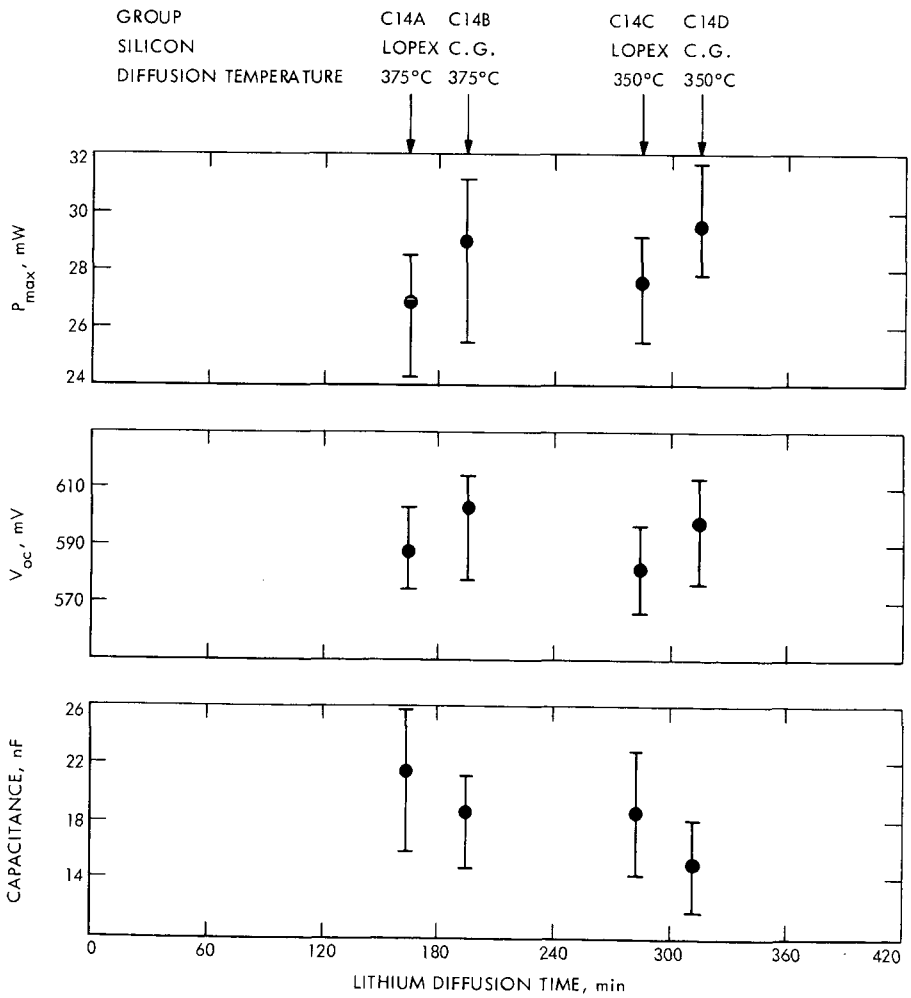

Fig. 13. Average values and spread of P_{max}, V_{oc}, and capacitance for C14 cell groups

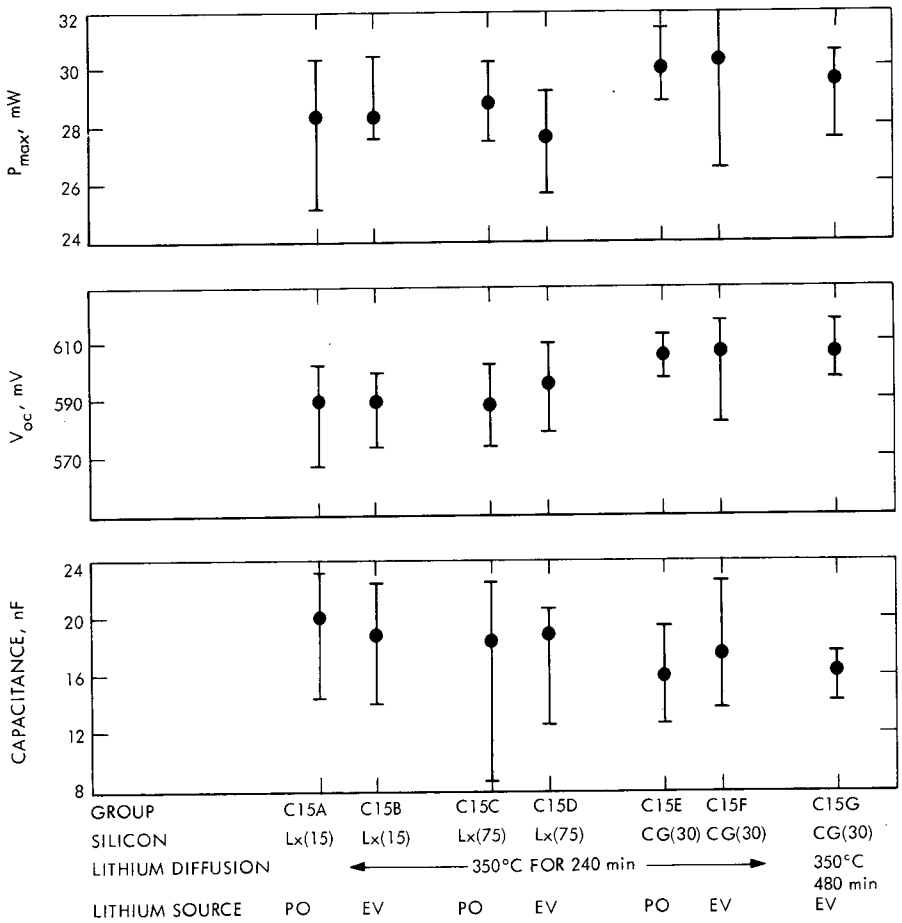

Fig. 14. Average values and spread for P_{max}, V_{oc}, and capacitance for C15 cell groups

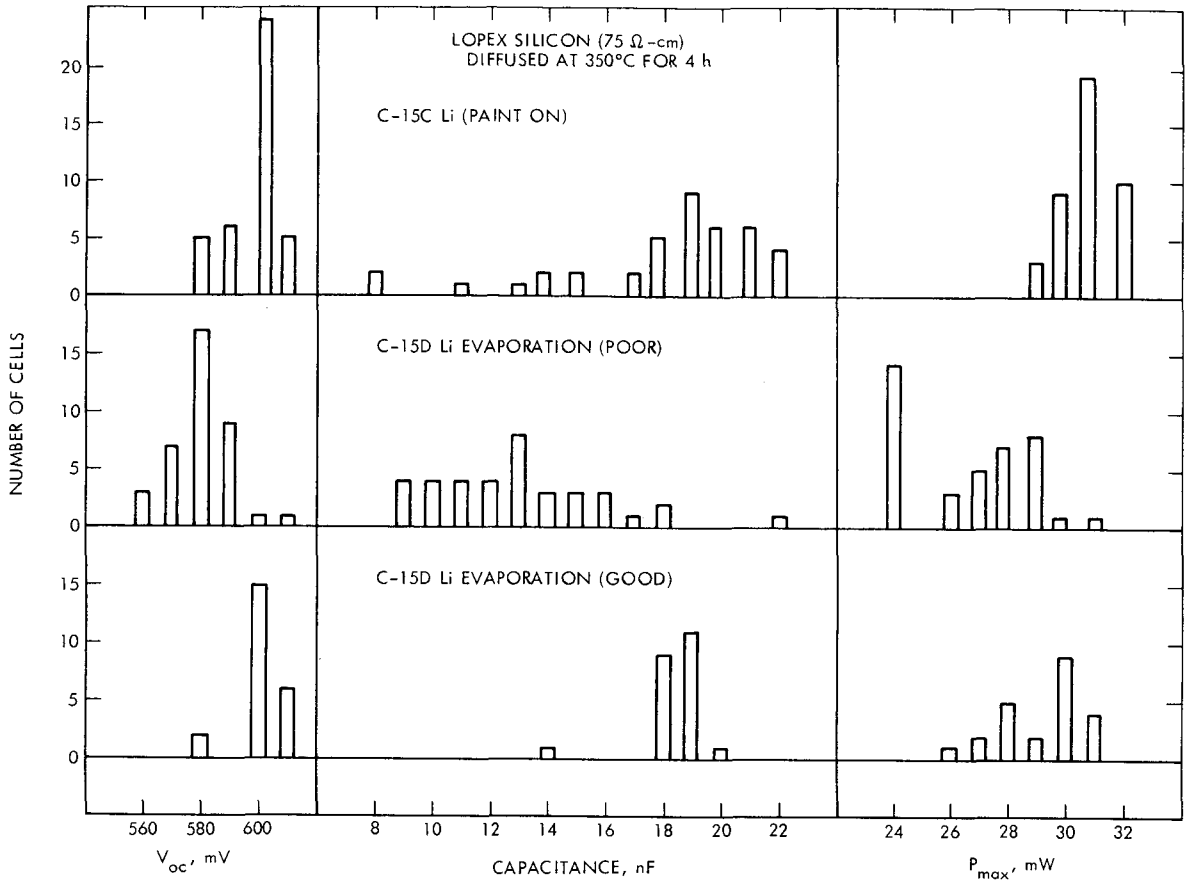

Fig. 15. Histogram plots of V_{oc}, capacitance, and P_{max} for three different conditions of lithium application in two C15 groups

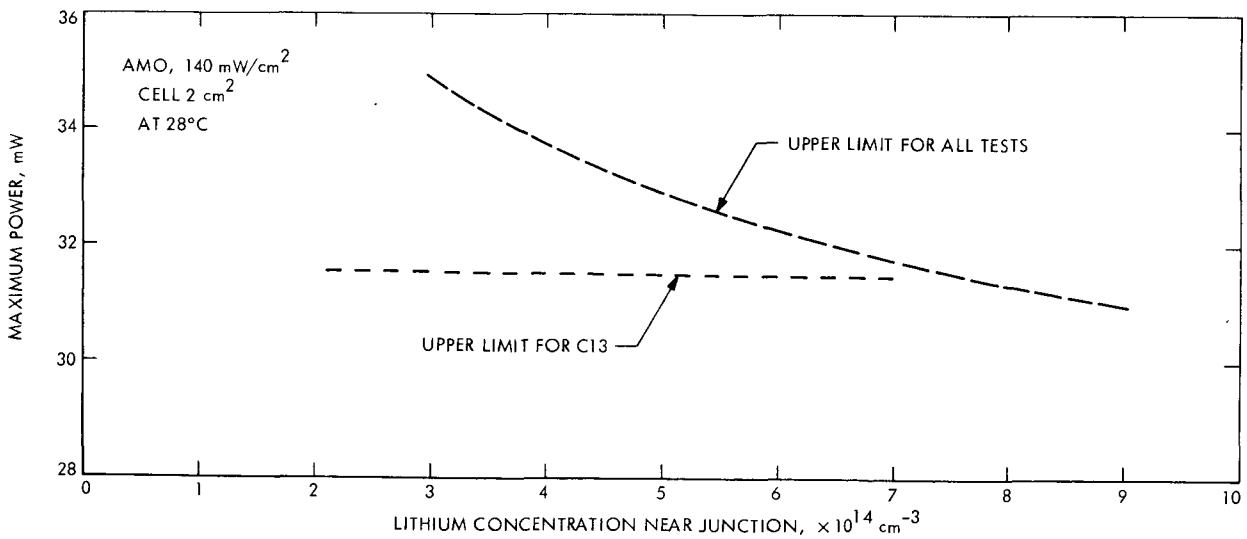

Fig. 16. Highest observed pairs of values for P_{max} and lithium concentration